APPENDIX C - TURBINE MISSILE STUDY

TABLE OF CONTENTS

APPENDIX C - TURBINE MISSILE STUDY

LIST OF TABLES

APPENDIX C - TURBINE MISSILE STUDY

LIST OF FIGURES

C.0 ABSTRACT

This appendix discusses the analyses that have been performed and inspection criteria which have been developed to show that the Byron/Braidwood Stations are acceptably safe against postulated turbine missile damage. These missiles result from a postulated high pressure turbine rotor fracture and a low-pressure turbine disk fracture at design and destructive overspeeds.

C.0.1 Current Approach

Byron/Braidwood currently use the probability values outlined in Reference 6 and reproduced in Table C.0-1 for the minimal acceptable range which will allow unit startup or continued operation. The stations fall into the Unfavorably Oriented category. To ensure the Byron/Braidwood turbine rotors maintain their integrity and unit operation is maintained within the SER limits a probabilistic program based on the manufacturers' methodology has been implemented.

The method uses manufacturer supplied missile generation probability values, P_1, for each low pressure turbine rotor. The missile generation probability values are provided for both rated speed and overspeed conditions for different operational lengths of time. For each individual turbine rotor the overspeed and rated speed probability values are added together, giving the total probability of a missile generation based on time in operation. This information is generally displayed in graphical form. Each time a rotor disc inspection is performed and the results are satisfactory (no indications found within the rotor disc which could lead to disc rupture) the operational point on the time vs missile generation curve is set back to zero hours of operation.

At each refueling outage a calculation for total unit missile generation probability is made. To make this calculation the operational hours on each of the low pressure turbines is gathered. The missile generation probability for each of the LP turbine rotors is taken from the individual rotor's graph based on the operational time on the rotor. The values for the three rotors are then added together to determine the current missile generation probability for the unit. This value must be below 1.0E-05 to allow loading the turbine and bringing the unit on line.

In addition, a calculation is made to determine when the unit missile generation probability will drop below the point at which action (rotor inspection) must be taken. This calculation is made using the three individual rotor curves and the operation hours on each of the turbine rotors. A curve is usually generated. From this combined curve the total

length of operational time allowable before action must be taken is determined. This value is compared against the duration of the next fuel cycle to ensure a forced shutdown will not occur.

If a turbine rotor is replaced, or if indications during disc inspections are found which require replacement or maintenance, new probability values will be supplied by the rotor manufacturer. The probabilistic determination method described above would then be performed to ensure missile generation probabilities are within an acceptable range and that no forced shutdown would occur in the next fuel cycle.

This approach focuses on the probability of turbine missile generation, P_1, which is consistent with the recommendations provided in Reference 6. The emphasis was shifted from determining strike and damage probabilities (P_2 and P_3), which involved elaborate and ambiguous analyses, to the probability of turbine failure resulting in the ejection of turbine disc (or internal structure) fragments through the turbine casing (P_1). The NRC has since reviewed and approved the manufacturer's (Westinghouse) methodology which provides procedures for estimating crack growth, missile generation (P_1), and volumetric inspection intervals (Reference 8). The following is a discussion of previous approaches used to satisfy turbine missile protection requirements.

C.0.2 Previous Approach

According to Bush (Reference 1) the probability per year (P_4) of turbine missile damage may be expressed as

$$P_4 = P_1 \cdot P_2 \cdot P_3$$

where:

P_1 = Probability of turbine failure resulting in the ejection of a missile, per year.

P_2 = Probability that a missile will strike a barrier which houses a critical plant component, given that a missile has been ejected from the turbine; and

P_3 = Probability that a missile will perforate a barrier, thus damaging a critical plant component, given that a missile has been ejected from the turbine and has struck the barrier.

Based on studies conducted by Twisdale et al. (Reference 5), the product of $(P_2)(P_3)$ can be taken as 10^{-3} or 10^{-2} depending upon favorable or unfavorable turbine orientation, respectively. Thus, the probability, P_1, of a turbine failure

resulting in ejection of a missile must meet the guidelines given in Table C.O-1 taken from Reference 3. The methodology for evaluation of P_1 values at that time had been submitted to but not yet reviewed by the NRC.

It is also specified in Reference 6 that until approval of the methodology two criteria must be met regardless of turbine orientation. These criteria are:

a. Having an inservice inspection program of the steam turbine rotor acceptable to the NRC that will provide assurance that disk flaws having potential for brittle failure of a disk at speeds up to design speed will be detected.

b. Having an inservice inspection and test program for the governor and overspeed protection system that is acceptable to the NRC for detection of failures that can lead to overspeed conditions above the design overspeed.

The inspection program to meet these two criteria was submitted in Reference 7 for review. Until a program was approved, volumetric inspection of all low pressure turbine rotors was required to be performed every third refueling outage and an acceptable turbine valve inspection program was incorporated Technical Requirements Manual 3.3.g. Subsequently, the NRC has reviewed and approved a program as outlined in Section C.0.1.

C.0.3 Original Approach

The remainder of this appendix discusses the original approach where the strike and damage probabilities, P_2 and P_3, were calculated. This work has been superseded by the approach summarized in Section C.0.1. The following sections of this appendix are included for historical purposes.

TABLE C.0-1

RELIABILITY CRITERIA

	PROBABILITY, YR^{-1}		
	FAVORABLY ORIENTED	UNFAVORABLY ORIENTED	REQUIRED LICENSEE ACTION
A.	$P_1 < 10^{-4}$	$P_1 < 10^{-5}$	This is the general, minimum reliability requirement for loading the turbine and bringing the system on line.
B.	$10^{-4} < P_1 < 10^{-3}$	$10^{-5} < P_1 < 10^{-4}$	If during operation this condition is reached, the turbine may be kept in service until the next scheduled outage, at which time the licensee is to take action to reduce P_1 to meet the appropriate A criterion (above) before returning the turbine to service.
C.	$10^{-3} < P_1 < 10^{-2}$	$10^{-4} < P_1 < 10^{-3}$	If during operation this condition is reached, the turbine is to be isolated from the steam supply within 60 days, at which time the licensee is to take action to reduce P_1 to meet the appropriate A criterion (above) before returning the turbine to service.
D.	$10^{-2} < P_1$	$10^{-3} < P_1$	If at any time during operation this condition is reached, the turbine is to be isolated from the steam supply within 6 days, at which time the licensee is to take action to reduce P_1 to meet the appropriate A criterion (above) before returning the turbine to service.

C.1 INTRODUCTION

This report examines the Byron/Braidwood Stations for susceptibility to damage due to a catastrophic failure of the turbine generator, resulting in the ejection of high-speed rotor fragments, hereafter called "turbine missiles." The probability is calculated of turbine missiles causing damage that interferes with normal safe shutdown or damage that results in environmental releases beyond the limits specified by 10 CFR 100 during normal operating or safe shutdown conditions.

In Section C.2, the methodology used to determine the probability of turbine missile damage is presented. In Section C.3, numerical values are assigned to the parameters of the analysis, and features unique to the Byron/Braidwood Stations are discussed. The results of the analysis and a summary are presented in Sections C.4 and C.5, respectively.

C.2 METHODOLOGY

The probability of turbine missile damage is expressed (after Bush, Reference 1) as:

$$P_4 = P_1 \cdot P_2 \cdot P_3 \qquad \text{(C.2-1)}$$

where:

P_4 = probability of turbine missile damage, per year;

P_1 = probability of turbine failure resulting in the ejection of a missile, per year;

P_2 = probability that a missile will strike a barrier which houses a critical plant component, given that a missile has been ejected from the turbine; and

P_3 = probability that a missile will penetrate a barrier, thus damaging a critical plant component, given that a missile has been ejected from the turbine and has struck the barrier.

P_1, P_2 and P_3 are evaluated using a method which considers turbine characteristics, turbine failure mechanisms, plant layout, barrier types, and the inherent variability of the parameters influencing missile penetration. A description of the method follows.

C.2.1 P_1 - Missile Generation Probability

The general process for the generation of a missile begins when the generator separates from the system and because of a succession of malfunctions in the protection system, the steam supply to the turbines is not properly interrupted. The turbine is subsequently driven to an overspeed condition at which one of the discs breaks into several pieces, some of which perforate the turbine housing and become known as missiles.

In general, two specific overspeed conditions are of interest:

a. Design Overspeed: This is 120% of rated speed and is based on the precept that should the turbine speed governing system be incapacitated so that the turbine is tripped by the overspeed trip mechanism, the calculated speed attained will not exceed 120% of rated speed.

b. Destructive Overspeed: The bursting speed of each shrunk-on disc is calculated. The criterion used is that the disc will fail when the average tangential stress equals the maximum ultimate tensile

strength of the disc material. Disc No. 3 is the most highly stressed disc, with a calculated failure speed of 182% of rated speed. Upon failure of disc No. 3, further acceleration of the unit is assumed to halt, and for the purpose of analysis, all other discs have been assumed to fail at 182% of rated speed.

At either overspeed condition, it is assumed that the rupture of one disc will do sufficient damage to the unit such that further overspeeding and additional missile generation will not occur. It is further assumed that the disc will rupture into four quadrants, of which two will be projected downward into the turbine foundation, one will be projected toward the plant, and one will be projected away from the plant. If the disc ruptures into fewer than four pieces, the probability that one of the pieces will be projected toward the plant will be less than unity. If the disc ruptures into more than four pieces, each piece will have proportionately less mass and, therefore, less potential for damage.

The determination of the probability of generating a turbine missile is an extremely complex problem that can be, and has been, stated in various ways with a resulting variety of answers.

For further discussion of this problem, see Reference 2.

C.2.2 P_2 - Strike Probability

The method of determining the strike probability, P_2, has been adopted from Reference 2 and is summarized here.

If a missile is produced by a rupturing disc, it will leave the turbine with a given speed and direction, where the direction can be defined in terms of two angles, i.e., the angle from the horizontal plane and the angle of the horizontal component from the turbine axis. This three-dimensional space (speed and two angles) is called the exit dynamics space. A given target has an "image" in the exit dynamics space which consists of all points, i.e., initial speed and direction, which result in the missile hitting the target. The basic problem is to describe this image in terms of the target position, orientation, and size. This is done only for plane targets, since any target can be subdivided into "subtargets" which are small enough to be approximated by plane targets.

The first problem considered is that of finding the image of a given point target. This result is extended to the case of a target consisting of a short line passing through the point at an arbitrary angle in the plane of the trajectory, and then to the case of a plane target with an arbitrary orientation. The final result is an expression for the image of a plane target of given orientation and size located at a given position.

Consider the coordinate system shown in Figure C.2-1. The origin is the center of the disc which ruptures, the x-axis corresponds to the turbine axis, and the disc rotates in the y-z plane. The missile will leave the origin with an initial speed v and initial direction defined by θ_o and ϕ_o (see Figure C.2-1). For a given point (x_o, y_o, and z_o) the objective is to find the combinations (v, ϕ, θ) which will result in the trajectory of the missile passing through the point.

Since the only force acting on the missile is that of gravity (air resistance is ignored), the trajectory will lie in the plane $\theta = \theta_o$, where

$$\theta_o = \tan^{-1} (x_o / y_o) \qquad \text{(C.2-2)}$$

and the original problem reduces to a two-dimensional problem. If ρ is the distance from the origin along the intersection of the x-y plane and the $\theta = \theta_o$ plane, then the problem is as shown in Figure C.2-2,

$$\rho_o = \sqrt{x_o^2 + y_o^2} \qquad \text{(C.2-3)}$$

The equation of the trajectory in the ρ-z plane is

$$z = \rho \tan \phi - (g \rho^2 / 2 v^2 \cos^2 \phi) \qquad \text{(C.2-4)}$$

Where g is the acceleration of gravity. For a given (ρ_o, z_o) the equation can be solved for v as a function of ϕ obtaining

$$v = \rho_o \sqrt{g/2 \cos^2 \phi(\rho_o \tan\phi - z_o)} \qquad \text{(C.2-5)}$$

and from this it follows that ϕ is restricted to the range

$$\tan^{-1}\left(\frac{z_o}{\rho_o}\right) < \phi < 90° \qquad \text{(C.2-6)}$$

It can also be shown that v is restricted to the range

$$v \geq \sqrt{g (z_o + \sqrt{\rho_o^2 + z_o^2})} \qquad \text{(C.2-7)}$$

Figure C.2-3 is a graph of v vs. ϕ. This is the image in the exit dynamics space of the point target.

Next, consider a small line target centered at (ρ_o, z_o) of length Δ_1 at an angle ξ with respect to the horizontal

$$(-\frac{\pi}{2} \leq \xi \leq \frac{\pi}{2})$$

as shown in Figure C.2-4. For each value of ϕ satisfying Equation C.2-6 in Figure C.2-3 there will be a range of values for v which will result in the line target being hit by the missile. Using a differential argument with Equation C.2-5, the range in v, dv, is given by

$$dv = \sqrt{\frac{g}{2\cos^2\phi}} \left[\frac{\rho_o(\sin\xi + \cos\xi\tan\phi) - 2z_o\cos\xi)}{2(\rho_o\tan\phi - z_o)^{3/2}}\right]\Delta_1 \qquad (C.2\text{-}8)$$

In the ϕ - v plane the line of allowable values in Figure C.2-3 for a point target becomes a band of allowable values for the line target, as shown in Figure C.2-5. Equation C.2-8 is an approximation whose accuracy is a function of the size of Δ_1. The less the expression in square brackets in Equation C.2-8 changes over the line, the more accurate is the approximation.

Because of the nature of the physical problem, only those trajectories are of interest which result in the missile hitting the target from the positive side, i.e., the side from which the upward pointing normal vector N = (-sin ξ, cos ξ) extends. This condition is stated mathematically by requiring that the dot product of the velocity $\bar{v}$ and $\bar{N}$ be negative. This leads to the restriction:

$$\phi > \tan^{-1}\left(\frac{2z_o}{\rho_o} - \tan\xi\right) \qquad (C.2\text{-}9)$$

If $\tan\xi \geq z_o/\rho_o$ then Equation C.2-9 is less restrictive than Equation C.2-6 and has no effect on the allowable range of ϕ.

Next consider an area centered at (x_o, y_o, z_o), or equivalently at (ρ_o, z_o, θ_o), whose orientation is defined by its normal vector N = (cosα, cosβ, cosγ), where α, β, and γ are the direction cosines of N, as shown in Figure C.2-6. The line of intersection of the target area and the ρ-z plane, L_1, is the line which corresponds to the line Δ_1 in Figure C.2-4. It can be shown that the slope of this line in the ρ-z plane is given by

$$\tan\xi = -\frac{(\sin\theta\cos\alpha + \cos\theta\cos\beta)}{\cos\gamma} \qquad (C.2\text{-}10)$$

With this angle, Equation C.2-8 can be used to calculate the band of allowed values in the ϕ-v plane, as shown in Figure C.2-5.

Let L_2 be the line in the target plane which is perpendicular to L_1. The extent of the target in this direction must be covered by varying θ through an angle $d\theta$. If $n = (\cos\theta, -\sin\theta, 0)$ is the normal to the ρ-z plane then L_2 is a scalar multiple of $\bar{N} \times (\bar{N} \times \bar{n})$, where

$$\begin{aligned}\bar{N} \times (\bar{N} \times \bar{n}) = [&- \sin\theta \cos\alpha \cos\beta - \cos\theta \\ &(\cos^2\beta + \cos^2\gamma)]\,\bar{i} \\ &+ [\sin\theta (\cos^2\alpha + \cos^2\gamma) + \\ &+ \cos\theta \cos\alpha \cos\beta]\,\bar{j} \\ &+ [\cos\gamma (\cos\theta \cos\alpha - \sin\theta \cos\beta)]\,\bar{k}\end{aligned} \qquad \text{(C.2-11)}$$

and $\bar{i}$, $\bar{j}$, $\bar{k}$ are the unit vectors in the x, y, and z directions, respectively. $\bar{L}$ is defined to be the unit vector in this direction

$$\bar{L} = \frac{\bar{N} \times (\bar{N} \times \bar{n})}{|| \bar{N} \times (\bar{N} \times \bar{n}) ||} \qquad \text{(C.2-12)}$$

and the projection of $\bar{L}$ onto $\bar{N}$ is to be found.

$$\bar{L}.\bar{n} = \frac{- 2 \sin\theta \cos\theta \cos\alpha \cos\beta - \sin^2\theta \cos^2\alpha - \cos^2\theta \cos^2\beta - \cos^2\gamma}{|| \bar{N} \times (\bar{N} \times \bar{n}) ||} \qquad \text{(C.2-13)}$$

If the dimension of the target area along L_2 is Δ_2 then $d\theta$ must satisfy

$$\rho_o \, d\theta = | \bar{L}.\bar{n} | \, \Delta_2 \qquad \text{(C.2-14)}$$

or

$$d\theta = \frac{| \bar{L}.\bar{n} | \, \Delta_2}{\rho_o} \qquad \text{(C.2-15)}$$

If Fig. C.2-5 is extended to three dimensions by letting the θ-axis come out of the page, the shaded area of allowable values takes on a thickness in the θ-direction of $d\theta$ given by Equation C.2-15.

The above projection replaces the original target area by its projection on the plane determined by L_1 and n, and to this extent it is an approximation. This should be a reasonable approximation as long as ρ and ξ do not change appreciably over the area.

Now assume that the initial velocity and direction of the missile are random variables. The initial velocity and direction are specified by three independent random variables: the random variable v representing the initial velocity, the random variable θ_1 representing the angle of the vertical component (i.e., the projection on disc plane) from the horizontal plane, and the random variable θ_2 representing the angle from the disc plane (see Figure C.2-7). Assume that:

a. The initial velocity v is uniformly distributed between v_1 and v_2, where $v_1 < v_2$.

b. The angle θ_1 is uniformly distributed between 0 and $\pi/2$ for one quadrant.

c. The angle θ_2 is uniformly distributed between $-\Delta^\circ$ and $+\Delta^\circ$.

(If θ_2 is uniform between θ_{min} and θ_{max}, the strike probability can be obtained by using the following formula:

$$P_2 = \frac{\theta_{max}}{\theta_{max} - \theta_{min}} P[\theta_{max}] - \frac{\theta_{min}}{\theta_{max} - \theta_{min}} P[\theta_{min}]$$

where $P[\theta_{max}]$ and $P[\theta_{min}]$ are the strike probabilities obtained based θ_2 uniform between $-\theta_{max}$ and $+\theta_{max}$ and θ_2 uniform between $-\theta_{min}$ and $+\theta_{min}$, respectively.)

The probability of a missile having the initial velocity and direction within a specified range R (R is such that the missile will strike the target) can formally be written as:

$$P_2 = \text{Prob}\left[(\theta_1, \theta_2, v)\varepsilon R\right] = \int\int\int_{(\theta_1,\theta_2,v)\varepsilon R} f(\theta_1, \theta_2, v)\, dv d\theta_2 d\theta_1 \qquad \text{(C.2-16)}$$

where the probability density $f(\theta_1, \theta_2, v)$ has the form

$$f(\theta_1, \theta_2, v) = \begin{cases} \dfrac{1}{\frac{\pi}{2}(2\Delta)(v_2 - v_1)} & , \text{if } v_1 < v < v_2, 0 < \theta_1 < \dfrac{\pi}{2}, -\Delta < \theta_2 < \Delta, \\ 0 & , \text{otherwise}, \end{cases} \qquad \text{(C.2-17)}$$

since the random variables v, θ_1 and θ_2 were assumed to be uniformly distributed between v_1 and v_2, 0 and $\pi/2$, and $-\Delta$ and $+\Delta$, respectively. The distributions and Equation C.2-16 are expressed in terms of θ_1, θ_2, and v, which are hereafter called the distribution space, but the target, the missile trajectory, and its "image" are all expressed in the exit dynamics space. The exit dynamics space consists of the exit velocity v, the angle ϕ from the horizontal plane, and the angle θ of the horizontal component from the disc plane. The relationship between the distribution space and the exit dynamics space is given in Figure C.2-7. In order to be consistent, Equation C.2-16 is rewritten using the coordinates of the exit dynamics space:

$$P_2 = \text{Prob}\,[(\phi, \theta, v) \varepsilon\, R'] = \int\int\int_{(\phi,\theta,v)\varepsilon\, R} g(\phi, \theta, v)\,|J|\,dv\,d\theta\,d\phi \qquad \text{(C.2-18}$$

where $g(\phi,\theta,v) = f[\theta_1(\phi,\theta), \theta_2(\phi,\theta), v]$ (in this particular case, $g(\phi,\theta,v) = f(\theta_1,\theta_2,v)$ since $f(\theta_1,\theta_2,v)$ of Equation C.2-17 is independent of θ_1 and θ_2), R' in the exit dynamics space corresponds to R in the distribution space, and J is the Jacobian of transformation:

$$J = \frac{\partial(\theta_1, \theta_2, v)}{\partial(\phi, \theta, v)} = \frac{\partial(\theta_1, \theta_2)}{\partial(\phi, \theta)}$$

The expressions for J, $\theta_1(\phi,\theta)$ and $\theta_2(\phi,\theta)$ can be obtained from the relationships between (θ_1,θ_2) and (ϕ,θ):

$$\tan\theta_1 = \tan\phi \sec\theta,$$

$$\sin\theta_2 = \cos\phi \sin\theta. \qquad \text{(C.2-19)}$$

The Jacobian of transformation has the form:

$$|J| = \frac{(1 + \sin^2\phi \tan^2\theta)}{|\cos\phi|\,(1 + \tan^2\phi \sec^2\theta)\sqrt{1 - \cos^2\phi \sin^2\theta}} \qquad \text{(C.2-20)}$$

Suppose that the turbine disc is located at the origin and the disc plane coincides with $\theta = 0$ plane and that a target plane of dimensions Δ_1 by Δ_2 is specified by the location of its center (ρ_o, θ_o, z_o) in cylindrical coordinates and its orientation is specified by its normal vector $\bar{N} = (\cos\alpha, \cos\beta, \cos\gamma)$. The ranges of v, θ and ϕ which will hit the target can then be determined based on the relationships obtained earlier in this section. The probability of hitting the above specified target is given by the integral of the form in Equation C.2-18 with the proper limits of integration, which are determined by the location of the target, its size, and its orientation. In order to evaluate the integral of Equation C.2-18, the inner double integral of Equation C.2-18 is replaced:

$$\int\int_{(\theta,v)} g(\phi, \theta, v) \mid J \mid dv\, d\theta \quad \text{with} \quad g(\phi, \theta, v) \mid J \mid \Delta v \Delta\theta, \tag{C.2-21}$$

where

$$\Delta v = \sqrt{\frac{g}{2\cos^2\phi}} \left[\frac{\rho_o(\sin\xi + \cos\xi\tan\phi) - 2z_o\cos\xi)}{2(\rho_o\tan\phi - z_o)^{3/2}}\right] \Delta_1,$$

from Equation C.2-8, and

$$\Delta\theta = \frac{\mid \bar{L}.\bar{n} \mid}{\rho_o} \Delta_2 \tag{C.2-22}$$

from Equation C.2-15 with $(\bar{L}.\bar{n})$ given by Equation C.2-13. The angle ξ in Equation C.2-21 is given by Equation C.2-10:

$$\tan\xi = -\frac{(\sin\theta_o\cos\alpha + \cos\theta_o\cos\beta)}{\cos\gamma} \tag{C.2-23}$$

Now, the multiple integral of Equation C.2-18 can be replaced by the following simple integral

$$P_2 = \int_{\phi} g[\phi, \theta, v(\phi)] \mid J \mid \Delta v \Delta\theta d\phi, \tag{C.2-24}$$

where

$$v(\phi) = \rho_o \sqrt{\frac{g}{2\cos^2\phi(\rho_o \tan\phi - z_o)}} \qquad \text{(C.2-25)}$$

and ϕ is restricted to the range

$$\tan^{-1}\left(\frac{z_o}{\rho_o}\right) < \phi < \frac{\pi}{2} \qquad \text{(C.2-26)}$$

Since only those trajectories which result in the missile hitting the target from above are of interest, there is another restriction on ϕ (from Equation C.2-9):

$$\phi > \tan^{-1}\left(\frac{2z_o}{\rho_o} - \tan\xi\right) \qquad \text{(C.2-27)}$$

The fact that the random variable θ_2 is uniformly distributed between $-\Delta°$ and $+\Delta°$, i.e., $-\Delta \le \theta_2 \le +\Delta$, places another restriction on ϕ, which depends on the θ values,

$$h(\theta) < \phi < \frac{\pi}{2} \qquad \text{(C.2-28)}$$

where

$$h(\theta) = \begin{cases} \sin^{-1}\sqrt{\cos^2\Delta - \dfrac{\sin^2\Delta}{\tan^2\theta}}, & \text{if } \Delta < \theta \le \dfrac{\pi}{2} \text{ or } -\dfrac{\pi}{2} \le \theta \le -\Delta, \\ 0, & \text{if } -\Delta \ge \theta \le \Delta \end{cases}$$

The limits of integration for the integral of Equation C.2-24 can now be obtained from the fact that the random variable v is uniformly distributed between v_1 and v_2, i.e., $v_1 \le v \le v_2$, and the restrictions of Equations C.2-26 through C.2-28 on the allowed ϕ values. Defining

$$\phi_{min} = \max\{\tan^{-1}\left(\frac{z_o}{\rho_o}\right), \quad \tan^{-1}\left(\frac{2z_o}{\rho_o} - \tan\xi\right), h(\theta_o)\}, \qquad \text{(C.2-29)}$$

then the integral of Equation C.2-24 can be rewritten as

$$P_2 = \int_{\phi_{\ell_1}}^{\phi_{u_1}} \int_{\phi_{\ell_2}}^{\phi_{u_2}} \{g[\phi, \phi, v(\phi)] \mid J \mid \Delta v \Delta \theta\} d\phi \qquad \text{(C.2-30)}$$

With an additional restriction $\phi > \phi_{min}$. In the integral of Equation (C.2-30, ϕ_{u_1} and ϕ_{ℓ_2} are obtained by solving Equation C.2-25 for ϕ with $v = v_1$ and ϕ_{ℓ_1} and ϕ_{u_2} are obtained by solving Equation C.2-25 for ϕ with $v = v_2$. In general, there are two values of ϕ satisfying Equation C.2-25 for each v (see Figure C.2-8); ϕ_{ℓ_1} is the smaller of the two ϕ values corresponding to v_2 and ϕ_{u_1} is the smaller of the two ϕ values corresponding to v_1. For a given value of v, one ϕ value satisfying Equation C.2-25 is given by

$$\phi = \frac{1}{2}(\psi + \sin^{-1} A) \qquad \text{(C.2-31)}$$

where

$$A = \frac{\left(\frac{g\rho_o^2}{v^2} + z_o\right)}{\sqrt{\rho_o^2 + z_o^2}} \qquad \psi = \sin^{-1} \frac{(z_o)}{\sqrt{\rho_o^2 + z_o^2}}$$

and the other ϕ value is given by

$$\phi = \frac{1}{2}(\pi + \psi - \sin^{-1} A) \qquad \text{(C.2-32)}$$

if $\mid A \mid > 1$ for some v, then there exists no solution for ϕ, and in particular if $\mid A \mid \geq 1$ for some v_1, we set $\phi_{u_1} = \phi_{\ell_2} = \frac{\pi}{4} + \frac{1}{2}\psi$.

In summary, the probability of hitting a target plane of small area $\Delta_1 \times \Delta_2$, whose center is located at (ρ_o, θ_o, z_o) with its orientation given by its normal vector $\bar{N} = (\cos\alpha, \cos\beta, \cos\gamma)$, is given by the integral of Equation C.2-30 with the limits of integration ϕ_{ℓ_1}, ϕ_{u_2} and ϕ_{ℓ_2} determined from Equations C.2-29, C.2-31, and C.2-32.

If the area of a target is large, the differential approximation form of Equations C.2-8 and C.2-15 cannot be used for the entire area. Therefore, the probability of hitting the target can be obtained by first dividing the target area into small targets, for each small target evaluating the integral of Equation C.2-30 in order to obtain the probability of hitting a small target, and then finally summing up all the probabilities of hitting small targets.

C.2.3 P_3 - Penetration Probability

The probability of penetration, P_3, is calculated using Petry's formula:

$$D = K_p \frac{W}{A} \log_{10}\left(1 + \frac{S^2}{215{,}000}\right) \qquad \text{(C.2-33)}$$

where

D = depth of penetration into "infinitely" thick concrete (ft),

K_p = penetration coefficient (ft^3/lb),

W = missile weight (lb),

A = cross-sectional area of missile (ft^2), and

S = missile strike speed (ft/sec).

For a finite thickness of concrete, T(ft), the depth of penetration, D' (ft), is given as

$$D' = D\left[1 + \exp\left(8 - \frac{4T}{D}\right)\right] \qquad \text{(C.2-34)}$$

Assume that "damage" occurs if

$$D' > C_1 T \qquad \text{(C.2-35)}$$

or

$$D > C_2 T \qquad \text{(C.2-36)}$$

where C_1, C_2 are constants, and are related to each other through Equation C.2-34.

The variables in Equation C.2-33 (i.e., K_p, W, A, S), are random; hence, for any given thickness of concrete, there is a finite probability, P_3, that the missile may damage the enclosed components. This probability is calculated as:

$$P_3 = P[D > C_2 T] \qquad \text{(C.2-37)}$$

It is assumed that K_p is normally distributed, with mean m_K and coefficient of variation $V_K = 0.10$. Similarly, it is assumed that W is normally distributed with mean m_W and coefficient of variation $V_W = 0.10$. Then, for given values of S and A, the mean and coefficient of variation of D are approximately:

$$m_D = m_K \frac{m_W}{A} \log_{10}\left[1 + \frac{s^2}{215{,}000}\right] \qquad \text{(C.2-38)}$$

$$V_D^2 = V_K^2 + V_W^2 \qquad \text{(C.2-39)}$$

Assuming that D is normally distributed, P_3 for a given T, S, and A is

$$P_3 = F_U\left[-\frac{C_2 T - m_D}{m_D \quad V_D}\right] \qquad \text{(C.2-40)}$$

where F_U denotes the cumulative distribution function of the standardized normal variate with zero mean and unit standard deviation.

However, S, and A are random variables, and Equation C.2-40 represents the probability of damage, given the values of S and A. Equation C.2-40 must be multiplied by the probability density functions of S and A, and then integrated over the possible regions of S and A. Thus,

$$P_3 = \int_S \int_A F_U\left[-\frac{C_2 T - m_D}{m_D \quad V_D}\right] f_A(a)\, f_S(s)\, da\, ds \qquad \text{(C.2-41)}$$

Since A is taken to be uniformly distributed between the minimum missile area (A_1 in ft^2) and the maximum missile area (A_2 in ft^2), the probability density function of A is

$$f_A(a) = \frac{1}{A_2 - A_1} \qquad \text{(C.2-42)}$$

with the limits of integration on A from A_1 to A_2.

The strike speed is derived from the principle of conservation of energy, and is found to be

$$S = \sqrt{V^2 - 2gz_o} \qquad \text{(C.2-43)}$$

The probability density function of S can now be obtained from Equation C.2-43, from the probability density function of V, and from the relation $f(y)dy = f(x)dx$, and is

$$f_S(s) = \frac{1}{V_2 - V_1}\left[\frac{s}{\sqrt{s^2 + 2gz_o}}\right] \qquad \text{(C.2-44)}$$

The integration limits on S are obtained from the integration limits on ϕ used in Equation C.2-30 by finding the equation for S as a function of ϕ. Combining equations C.2-43 and C.2-25, we obtain

$$S = \sqrt{\frac{\rho_o^{\,2} g}{2\cos^2\phi\,(\rho_o \tan\phi - z_o)}} - 2g\,z_o \qquad \text{(C.2-45)}$$

The limits of integration over S in Equation C.2-41 can be obtained as the two intervals $S_{\ell 1}$ to ${}^{S}u_1$, and $S_{\ell 2}$ to ${}^{S}u_2$, where these limits are obtained by substituting the values of ϕ_{u1}, ϕ_{ℓ_1}, $\phi_{\ell 2}$, and ϕ_{u_2}, respectively, into Equation C.2-45.

Furthermore, the probability of penetration, P_3, is calculated using the correction for the angle of impact of the missile with the barrier. Bush (Reference 1) suggests that the actual thickness divided by the square of the cosine of the angle of impact gives the effective thickness to be penetrated. The angle of impact, i.e., the angle between the velocity vector at impact and the normal to the target area, is easily determined. If S is the velocity at impact and δ is the angle of impact, then

$$\cos\delta = \frac{-\bar{N}\cdot\bar{S}}{||\bar{S}||} \qquad \text{(C.2-46)}$$

where the negative sign is included because N is defined to be the upward pointing normal. Upon substitution and simplification Equation C.2-43 becomes

$$\cos\delta = \frac{\cos\alpha\,\sin\theta + \cos\beta\,\cos\theta + (\frac{2z_o}{\rho_o} - \tan\phi)\cos\gamma}{\sqrt{1 + \frac{2z_o}{\rho_o} - \tan\phi^2}} \qquad \text{(C.2-47)}$$

C.3 PARAMETERS

Westinghouse Electric Corporation has calculated the probability, P_1, of turbine failure resulting in the ejection of a missile as 9.5×10^{-11} per year for design overspeed and 1.7×10^{-6} per year for destructive overspeed (Reference 2). The characteristics of the missiles were determined in Reference 3, and are given here in Table C.3-1, where the missile velocities are assumed to be uniformly distributed with 10% of the value given in the table.

The critical plant regions in this analysis are the auxiliary building, the fuel handling building, the reactor containment buildings and the purge rooms. The locations of these buildings with respect to the turbines are shown in Figure C.3-1.

The moisture separator reheaters (MSR; 153 inch OD x 1-1/2 inch shell thickness) partly shield the wall of the auxiliary building from low-trajectory missiles. The shielding effect of the MSR is taken into account by calculating whether or not the postulated missiles perforate the MSR, and if so, the residual velocities of the missiles are determined using the methods of Reference 4 (Stanford Research Institute Formula). There is a 1-foot, 8-inch structural concrete wall in front of the auxiliary building wall (L row) enclosing plant office services area. The residual velocity of the missile, V_r, as it perforates through this wall is calculated using modified Petry's formula as follows:

$$V_r = \sqrt{v_m^2 - [215000 \{10^{(TA/2K_p W)} - 1\}]^2}$$

This residual velocity of the missile, V_r, is used for impact on the auxiliary building wall.

In addition to the shielding provided by the MSR and the 1-foot, 8-inch wall in front of L row, the structures on the roof of the auxiliary building which house the diesel exhaust silencers provide partial shielding against low trajectory missile strikes on the containment building wall. The effect of this shielding is explained in detail in Attachment A.

The properties of the target structures are as follows:

K_p = 0.00325 ft^3/lb for the reactor containment buildings. (This value is obtained by increasing the 5500-psi design strength of the containment concrete by 25% to account for added strength due to both aging and the overdesign associated with the basic mix design).

K_p = 0.00405 ft^3/lb for all other buildings. (3500-psi concrete, increased 25% as above).

C_1 = 0.667 for nonmetal-backed concrete, namely the auxiliary building walls.

C_1 = 0.715 for concrete roofs supported by metal decking.

C_1 = 0.800 for the containment concrete, which is backed by the containment liner.

The calculation of the strike probabilities was performed for small areas (10 ft x 10 ft maximum size) within each critical plant region, and the results were added to give the total strike probability for the region. The strike and penetration probabilities were calculated for the exterior walls and roofs only. In order to account for the fact that the safety-related components housed inside the Safety Category I structures were not individually and separately modeled, the strike probability for the region has been multiplied by the critical component density factor assigned for the region to obtain the value of P_2. The criteria for assigning a critical component density factor were relative area (volume) of the safety-related components to the area (volume) of the region, redundancy of components, location of the components, direction of the missile, and importance of the components as to their safety function. With these considerations and after a detailed review of the layout drawings for piping, cable and ducts, a single value of the critical component density factor was assigned for the region. Table C.3-2 shows the critical component density factors for different regions.

TABLE C.3-1

CHARACTERISTICS OF LOW-PRESSURE TURBINE MISSILES
(Shear and Rotation Modes)

MISSILE	WEIGHT W (lb)	DEFLECTION ANGLE θ_2	DESIGN OVER-SPEED EXIT VELOCITY (ft/sec)	DESTRUCTIVE OVERSPEED EXIT VELOCITY (ft/sec)	MAXIMUM AREA, A_2 (ft^2)	MINIMUM AREA, A_1 (ft^2)
Disc No. 1 Quadrant	3095	± 5°	Contained	262	5.60	2.60
Blade Ring No. 1 Fragment	4200	± 5°	Contained	262	11.62	3.34
Disc No. 2 Quadrant	3501	± 5°	Contained	405	6.70	3.00
Blade Ring No. 2 Fragment	2174	± 5°	Contained	405	6.84	1.90
Disc No. 3 Quadrant	4229	± 5°	Contained	440	6.70	3.30
Blade Ring No. 3 Fragment	2843	± 5°	Contained	440	9.55	2.61
Disc No. 4 Quadrant	3380	± 5°	370	704	3.50	2.00
Disc No. 5 Quadrant	3459	± 5°	156	518	3.72	1.36
Disc No. 6 Quadrant	3503	± (5°-25°)	268	542	4.50	1.38

TABLE C.3-2

CRITICAL COMPONENT DENSITY FACTORS

REGION	ELECTRICAL S/S*	MECHANICAL S/S	MECHANICAL R/R*	HVAC S/S	TOTAL
Aux. Bldg. Region 1	0.08			0.10	0.18
Aux. Bldg. Region 2	0.09			0.10	0.19
Aux. Bldg. Region 3					0.0
Aux. Bldg. Region 4	0.11				0.11
Aux. Bldg. Region 5	0.11				0.11
Aux. Bldg. Region 6					0.0
Aux. Bldg. Region 7	0.09			0.10	0.19
Aux. Bldg. Region 8	0.08			0.10	0.18
Aux. Bldg. Region 9	0.03			0.10	0.03
Aux. Bldg. Region 10	0.15			0.10	0.25
Aux. Bldg. Region 11	0.15			0.34	0.49
Aux. Bldg. Region 12	0.30			0.37	0.67
Aux. Bldg. Region 13	0.30			0.37	0.67
Aux. Bldg. Region 14	0.15			0.34	0.49
Aux. Bldg. Region 15	0.15			0.10	0.25
Aux. Bldg. Region 16	0.03				0.03
Aux. Bldg. Region 17	0.05			0.11	0.16
Reactor Bldg. Unit 1		1.00			1.00
Reactor Bldg. Unit 2		1.00			1.00
S. Purge Room-S. Section	0.02				0.02
S. Purge Room-N. Section	0.05			0.08	0.13
N. Purge Room-S. Section	0.05			0.08	0.13
N. Purge Room-N. Section	0.02				0.02
Fuel Handling Bldg.			0.10		

*S/S: Equipment required for safe shutdown
R/R: Radioactive release in excess of 10 CFR 100 limits

C.4 RESULTS

The results of the analysis are summarized in Table C.4-1. Details of the analysis for the reactor containment building for the destructive overspeed condition are given in Appendix C.A. Since the results are tabulated by target, the values of P_2 and P_3 are the average values of all the missiles striking the target at different locations and different angles of incidence.

Taking full advantage of the geometric symmetry of the problem, the analysis is performed for the complete set of target regions, but only one of the two turbine units is used to send missiles to the target structures. The values of P_2, P_3 and P_4 for individual targets are the probabilities due to turbine Unit 1.

The individual probabilities due to turbine Unit 1 are summed at the bottom of Table C.4-1 and then multiplied by 2 to account for turbine Unit 2.

The bottom values of P_4 labeled "TOTAL" are the total probabilities of damage to the plant per year. The notation in Table C.4-1, 4.294-08, means 4.294×10^{-8}.

TABLE C.4-1

SUMMARY OF RESULTS FOR BYRON/BRAIDWOOD

TARGET NAME	CONCRETE THICKNESS (in.)	DESIGN OVERSPEED			DESTRUCTIVE OVERSPEED		
		P_2	P_3	P_4	P_2	P_3	P_4
Aux. Bldg. Roof Region 1	24	1.953-04	2.022-02	3.753-16	3.050-05	7.814-02	4.052-12
Aux. Bldg. Roof Region 20	24	2.721-04	2.019-02	5.219-16	4.243-05	7.814-02	5.636-12
Aux. Bldg. Roof Region 3	24	0.000-00	0.000-00	0.000-00	0.000-00	0.000-00	0.000-00
Aux. Bldg. Roof Region 4	24	3.972-05	6.151-02	2.321-16	1.892-05	7.790-02	2.506-12
Aux. Bldg. Roof Region 5	24	7.317-06	3.340-00	2.321-16	1.892-05	7.774-02	2.506-12
Aux. Bldg. Roof Region 6	24	0.000-00	0.000-00	0.000-00	0.000-00	0.000-00	0.000-00
Aux. Bldg. Roof Region 7	24	8.779-06	6.432-01	5.364-16	3.728-05	8.893-02	5.637-12
Aux. Bldg. Roof Region 8	24	7.693-06	5.571-01	4.071-16	1.988-05	1.199-01	4.052-12
Aux. Bldg. Roof Region 9	24	2.654-05	2.043-02	5.150-17	4.183-06	7.822-02	5.562-13
Aux. Bldg. Roof Region 10	24	2.918-04	2.040-02	5.655-16	4.594-05	7.821-02	6.107-12
Aux. Bldg. Roof Region 11	24	5.155-04	2.627-02	1.287-15	1.046-04	7.812-02	1.389-11
Aux. Bldg. Roof Region 12	24	1.990-04	6.158-02	1.164-15	9.481-05	7.798-02	1.257-11
Aux. Bldg. Roof Region 13	24	3.687-05	3.324-01	1.164-15	9.501-05	7.782-02	1.257-11
Aux. Bldg. Roof Region 14	24	1.953-05	6.939-01	1.288-15	1.048-04	7.800-02	1.390-11
Aux. Bldg. Roof Region 15	24	9.506-06	6.435-01	5.811-16	4.038-05	8.898-02	6.108-12
Aux. Bldg. Roof Region 16	24	1.055-06	5.575-01	5.587-17	2.729-06	1.199-01	5.562-13
Aux. Bldg. E. Wall Region 9	20+ 36	0.000-00	0.000-00	0.000-00	4.226-03	1.497-01	1.076-09
Aux. Bldg. E. Wall Region 10	20+ 36	0.000-00	0.000-00	0.000-00	4.069-02	1.442-01	9.979-09
Aux. Bldg. E. Wall Region 11	20+ 36	0.000-00	0.000-00	0.000-00	6.280-03	6.899-02	7.365-10
Aux. Bldg. E. Wall Region 12	20+ 36	0.000-00	0.000-00	0.000-00	7.965-06	0.000-00	0.000-00
Aux. Bldg. E. Wall Region 13	20+ 36	0.000-00	0.000-00	0.000-00	3.659-06	0.000-00	0.000-00
Aux. Bldg. E. Wall Region 14	20+ 36	0.000-00	0.000-00	0.000-00	2.056-06	0.000-00	0.000-00
Aux. Bldg. E. Wall Region 15	20+ 36	0.000-00	0.000-00	0.000-00	4.988-07	0.000-00	0.000-00
Aux. Bldg. E. Wall Region 16	20+ 36	0.000-00	0.000-00	0.000-00	3.084-08	0.000-00	0.000-00
Aux. Bldg. Roof Region 17	14	1.472-04	1.572-01	2.198-15	1.206-04	2.276-01	4.668-11
Fuel Handling Bldg. Roof	14	1.339-04	1.430-01	1.818-15	9.958-05	2.296-01	3.887-11
S. Purge Room - Southernmost Roof Portion	14	8.525-05	1.135-02	9.191-17	3.611-05	2.251-02	1.360-12
S. Purge Room - Northernmost Roof Portion	14	3.713-04	4.544-02	1.603-15	7.362-05	2.308-01	2.889-11
N. Purge Room - Southernmost Roof Portion	14	1.371-05	9.975-01	1.299-15	7.372-05	2.299-01	2.881-11
N. Purge Room - Northernmost Roof Portion	14	7.013-07	9.737-01	6.487-17	2.742-06	2.672-01	1.245-12

TABLE C.4-1 (Cont'd)

TARGET NAME	CONCRETE THICKNESS (in.)	DESIGN OVERSPEED			DESTRUCTIVE OVERSPEED		
		P_2	P_3	P_4	P_2	P_3	P_4
Reactor Bldg. Unit 1 - Vertical Walls	42	7.061-02	1.120-07	7.511-19	9.079-02	6.010-02	9.276-09
Reactor Bldg. Unit 1 - Dome	36	1.365-02	1.186-04	1.538-16	1.762-03	1.961-02	5.873-11
Reactor Bldg. Unit 2 - Vertical Walls	42	2.285-06	0.000-00	0.000-00	1.949-05	0.000-00	0.000-00
Reactor Bldg. Unit 2 - Dome	36	3.880-04	4.139-03	1.526-16	1.393-03	2.481-02	5.875-11
For one turbine unit				1.584-14			= 2.147-08
Total for two turbine units				x 2 = 3.168-14			x 2 = 4.294-08

C.5 CONCLUSION

The total probability of turbine missile damage is 4.3×10^{-8} per year, which is less than the acceptable value of 2.0×10^{-7} per year for the two units. It is, therefore, concluded that Byron and Braidwood are acceptably safe against postulated turbine missile damage.

The value of P_1 has been reduced based on the design of the digital EHC system. The probability per year for turbine missile damage has been reduced by an order of magnitude. Revised probabilities are given in Westinghouse WNA-CN-00056-GEN, Revision 3, "Reliability Calculation of the Ovation DEH Overspeed Trip Function." The values of P_4 shown in this attachment remain bounding.

C.6 REFERENCES

1. S. H. Bush, "Probability of Damage to Nuclear Components Due to Turbine Failure," Nuclear Safety 14 (3), pp. 187-201, May-June 1973.

2. Westinghouse Electric Corporation, "Analysis of the Probability of the Generation and Strike of Missiles From a Nuclear Turbine," March 1974.

3. Westinghouse Electric Corporation, "Turbine Missile Information for Design Overspeed and Destructive Overspeed," Letter from L. K. Koering to G. C. Kuhlman of Sargent & Lundy dated September 16, 1977.

4. "Interim Criteria for the Design of Structures for Missile Impact Effects," Sargent & Lundy Report No. SDDA 136, March 1975.

5. L. A. Twisdale, W. L. Dunn, and R. A. Frank, "Turbine Missile Risk Methodology and Component Code," EPRI Seminar on Turbine Missile Effects in Nuclear Power Plants, Palo Alto, California, October 25-26, 1982.

6. U.S. Nuclear Regulatory Commission, "Safety Evaluation Report Related to the Operation of Byron Station, Units 1 and 2," NUREG-0876, Supplement No. 5, October, 1984.

7. Letter from T. R. Tramm of CECo to H. R. Denton of NRC, "Byron Generating Stations Units 1 and 2, Braidwood Generating Stations, Units 1 and 2, Turbine Missiles," dated September 25, 1984.

8. Letter from B. J. Youngblood of NRC to D. L. Farrar of CECo, "Byron Unit 1 License Condition on Turbine Missiles," dated May 20, 1985.

ATTACHMENT C.A
DETAILS OF PROBABILITY CALCULATIONS
FOR THE
CONTAINMENT BUILDING

C.A DETAILS OF PROBABILITY CALCULATIONS FOR THE CONTAINMENT BUILDING

A detailed analysis for strike and penetration probabilities for the containment wall is presented herein. It is shown that the probabilities for the containment building wall in a destructive overspeed accident are

$$P_2 = 1.8 \times 10^{-1} \text{ (for two turbine units)}$$

$$P_3 = 6.0 \times 10^{-2}$$

and

$$P_4 = 1.86 \times 10^{-8}/\text{year}$$

A similar analysis was performed for the design overspeed accident, the results of which are given in Table C.A-1. A detailed description of the analysis for destructive overspeed which was performed to obtain the above values is given below.

The method of analysis used in this attachment is identical to that used in Appendix C. The portion of the containment building wall between elevations 497 feet 0 inch and 579 feet 0 inch is comprised of regions A, B, C, and D of Figure C.A-2. A plan of this area is shown in Figure C.A-1.

Region A (Elevation 562 feet 0 inch to Elevation 579 feet 0 inch)

In this region, P_3 is zero since none of the postulated turbine missiles are capable of penetrating the effective thickness of concrete in this region. Therefore, P_4 is zero for region A.

Region B (Elevation 539 feet 0 inch to Elevation 562 feet 0 inch

It is assumed that region B is not shielded by other structures, and that missiles ejected from the turbine may strike this region directly.

Region C (Elevation 515 feet 6 inches to Elevation 539 feet 0 inch)

This region is partially shielded by structures (enclosing the diesel exhaust silencers) on the roof of the auxiliary building. Of the 36 discs in the three LP sections of each turbine unit, only six are capable of striking and penetrating the containment building wall in region C. An analysis was performed for these six discs.

Region D (Elevation 497 feet 0 inch to Elevation 515 feet 6 inches)

This region is shielded from direct impact by the wall (3 feet 0 inch) and roof (2 feet 0 inch) of the auxiliary building.

None of the postulated missiles is capable of penetrating the effective thickness of this dual barrier. Therefore, in this region P_2 is zero; hence, P_4 is zero also.

The probability values for the above regions are tabulated in Table C.A-1. These values were computed on the basis of the assumptions discussed above, and utilizing the methodology described in the body of this report. The calculations were performed on MISLODS. MISLODS is a computer program developed by Sargent & Lundy to compute the probability of damage from turbine missiles.

An approximate check on the values of P_2 and P_3 for regions B and C follows. Differences between the approximate values computed below and the values from MISLODS are due primarily to the effect of the curvature of the containment building which is not considered in the approximate calculation.

$\underline{P_2}$

The probability that region B will be struck by a missile is approximately equal to the likelihood that a missile will be ejected into the 5.9° angle which encloses region B times the number of missiles which are ejected. For a single disc failure, the average number of missiles which will be ejected is 1.5 due to the fragments which are also ejected. Also one-third of the missiles originating from different LP sections of a turbine unit miss the containment. Therefore, P_2 for region B is approximately

$$2/3 \times 1.5 \times \frac{5.9^\circ}{90^\circ} = 6.55 \times 10^{-2}$$

which compares favorably with the value of 4.85×10^{2} computed by MISLODS.

P_2 for region C may be computed in a similar manner. However, due to the relative positions of region C, the structures on the roof of the auxiliary building, and the turbine discs, only six of the 36 discs can produce missiles which are capable of both striking region C and damaging the containment building. These six discs are shown in Figure C.A-1. From Figure C.A-2, the missiles must be ejected into a 6.8° "window" in order to strike region C. The resulting P_2 for region C is approximately

$$\frac{6}{36} \times \frac{6.8^\circ}{90^\circ} = 1.259 \times 10^{-2},$$

which compares favorably with the value of 1.072×10^{-2} computed by MISLODS.

$\underline{P_3}$

Figure C.A-3 is a plot of P_3 versus concrete thickness for quadrants from discs numbers 4, 5, and 6 in a destructive overspeed turbine failure. The angle of impact of the missile with the target is taken as 0° (i.e., direct impact). For oblique impact, the actual target thickness divided by the square of the cosine of the angle of impact gives the effective thickness to be penetrated. This effective thickness is taken as 4.81 feet for region B and 4.27 feet for region C. Knowing these effective thicknesses, the value of P_3 for each missile striking regions B and C can be obtained from the curves in Figure C.A-3. Table C.A-2 shows the computation of P_3 for regions B and C. The values obtained are in reasonable agreement with the values given by MISLODS.

TABLE C.A-1

PROBABILITIES FOR CONTAINMENT BUILDING WALL

REGION	P_1/yr	P_2	P_3	P_4/yr
A	1.7×10^{-6}	*	0	0
B	1.7×10^{-6}	8.007×10^{-2}	3.230×10^{-2}	4.4×10^{-9}
C	1.7×10^{-6}	1.072×10^{-2}	2.704×10^{-1}	4.9×10^{-9}
D	1.7×10^{-6}	0	*	0
				9.3×10^{-9}

For two units, $P_4 = 1.86 \times 10^{-8}$/year

*Not computed

TABLE C.A-2

APPROXIMATE COMPUTATION OF P_3 FOR REGIONS B AND C

MISSILE NUMBER i	DESCRIPTION	REGION B, T = 4.81 ft			REGION C, T = 4.27 ft		
		n_i	P_{3_i}	$n_i P_{3_i}$	n_i	P_{3_i}	$n_i P_{3_i}$
1	Disc No. 1 Quadrant	6	0.000	0.000	0	0.000	0.000
2	Blade Ring No. 1 Fragment	6	0.000	0.000	0	0.000	0.000
3	Disc No. 2 Quadrant	6	0.000	0.000	0	0.000	0.000
4	Blade Ring No. 2 Fragment	6	0.000	0.000	0	0.000	0.000
5	Disc No. 3 Quadrant	6	0.000	0.000	0	0.000	0.000
6	Blade Ring No. 3 Fragment	6	0.000	0.000	0	0.000	0.000
7	Disc No. 4 Quadrant	6	0.330	0.909	2	0.530	0.779
8	Disc No. 5 Quadrant	6	0.130	0.566	2	0.235	0.414
9	Disc No. 6 Quadrant	6	0.125	0.551	2	0.217	0.387
		54			6		

$\overline{P_{3_{AVE}}} = (1/54)\ (0.909 + 0.566 + 0.551) = 3.75 \times 10^{-2}$

$P_{3_{AVE}} = (1/6)\ (0.799 + 0.414 + 0.387) = 2.633 \times 10^{-1}$

Legend: n_1 = number of missiles of type i considered to be capable of striking the containment building wall in the region of interest.

P_{3_i} = P_3 for missile type i corresponding to the effective thickness of the containment building wall in the region of interest (obtained from curves in Figure C.A-3).

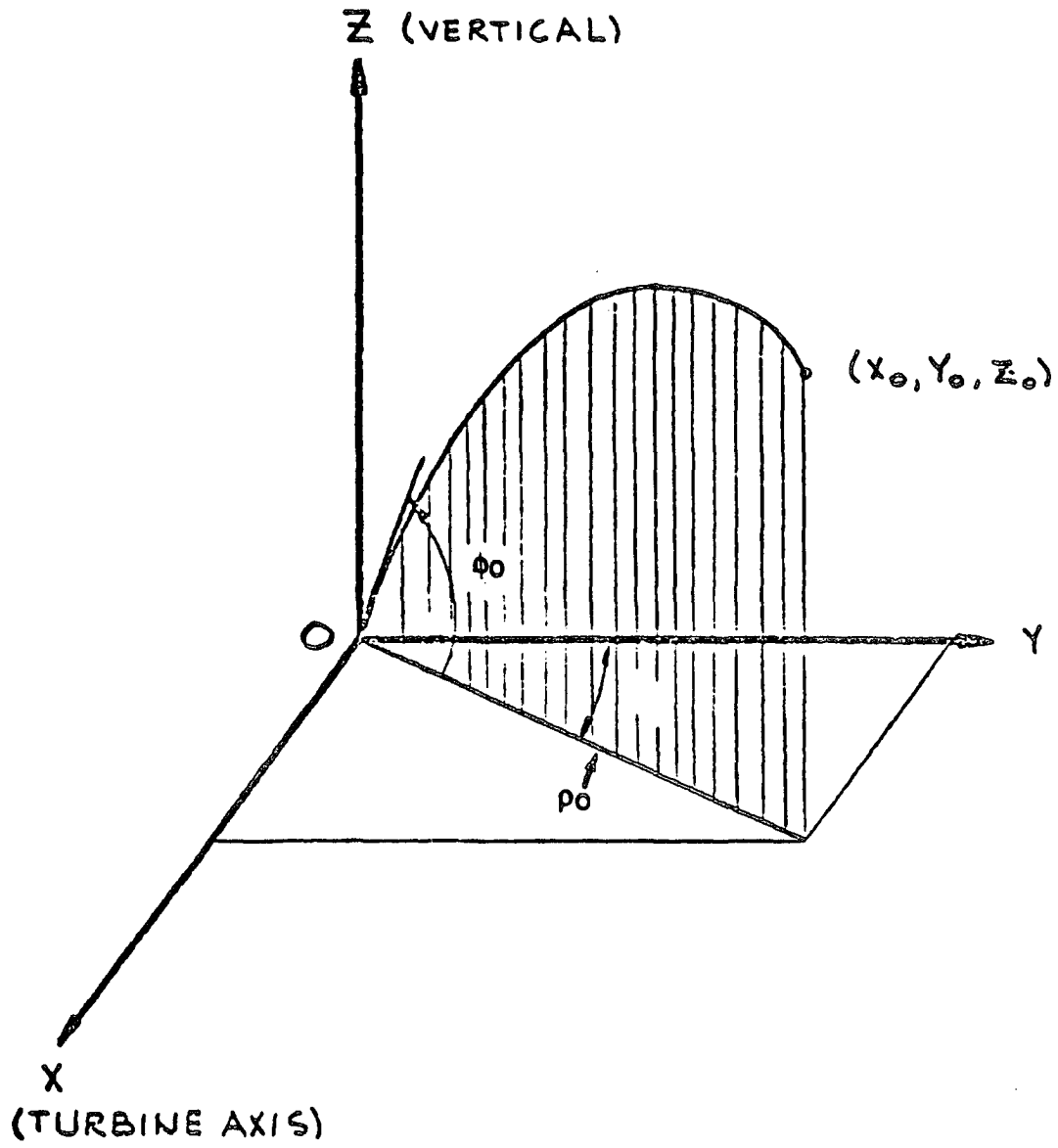

BYRON/BRAIDWOOD STATIONS UPDATED FINAL SAFETY ANALYSIS REPORT
FIGURE C.2-1 ASSUMED COORDINATE SYSTEM FOR THE MODEL

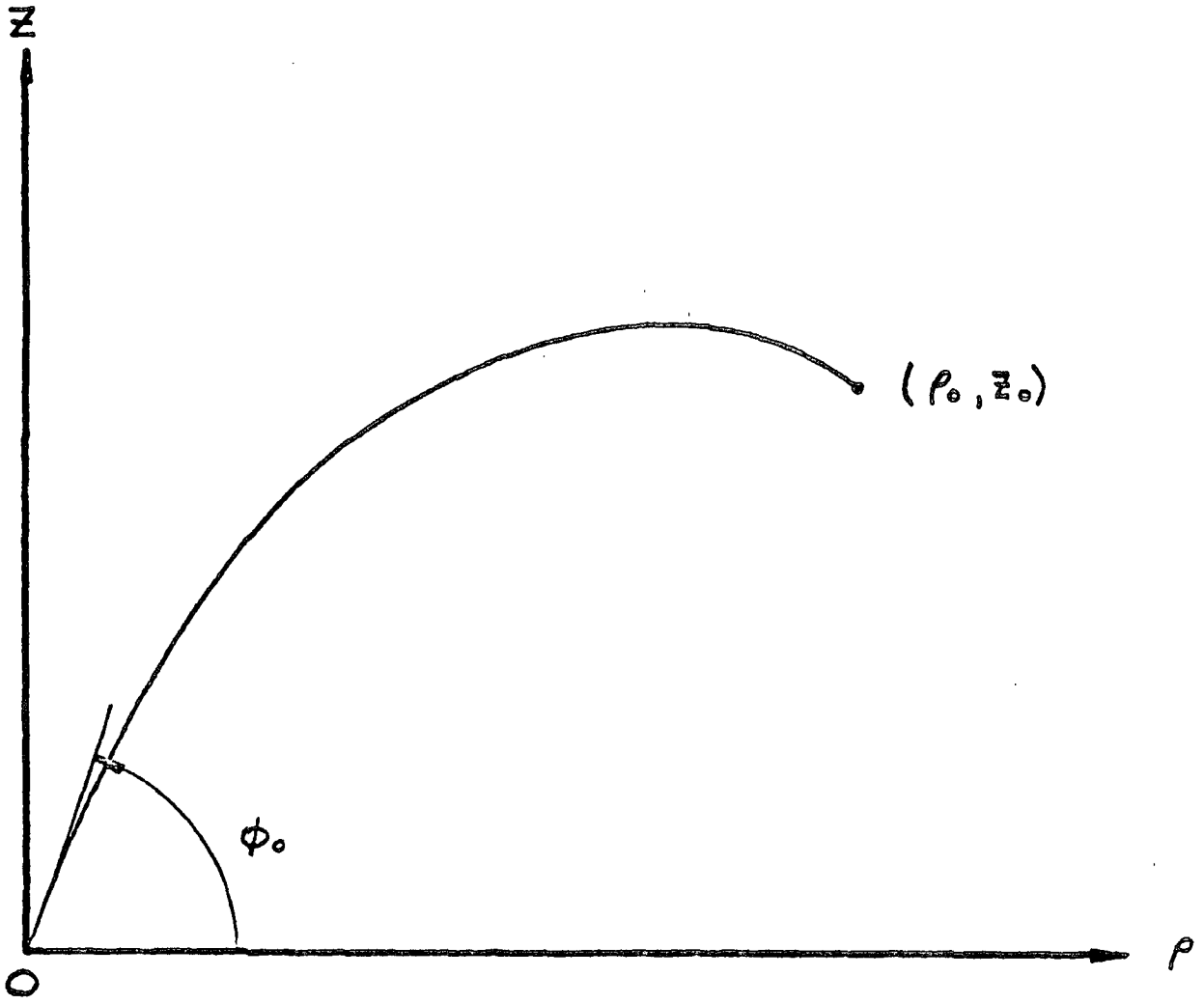

BYRON/BRAIDWOOD STATIONS
UPDATED FINAL SAFETY ANALYSIS REPORT

FIGURE C.2-2

TRANSFORMED TWO-DIMENSIONAL
COORDINATE SYSTEM

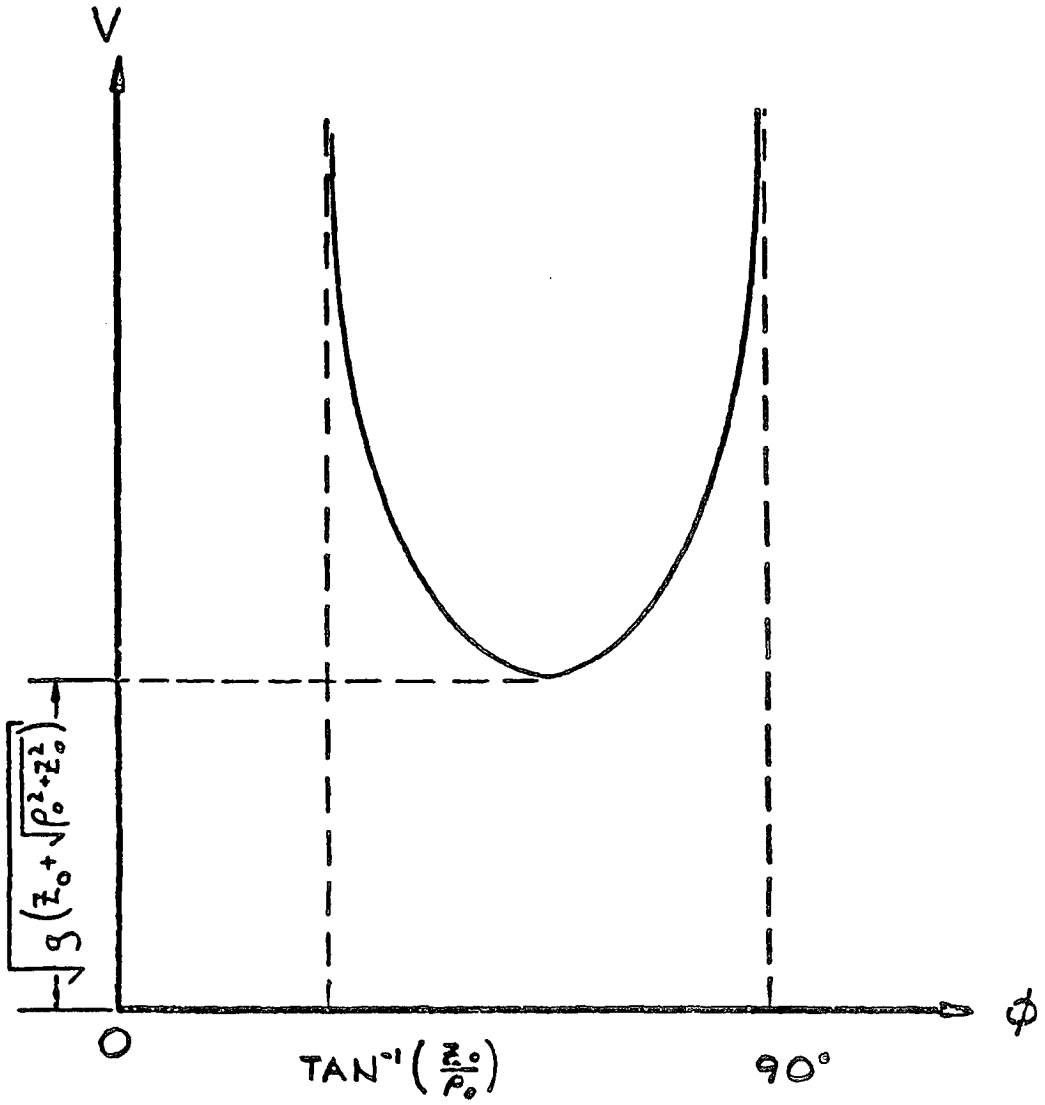

BYRON/BRAIDWOOD STATIONS UPDATED FINAL SAFETY ANALYSIS REPORT
FIGURE C.2-3 EXIT DYNAMICS SPACE OF THE POINT TARGET

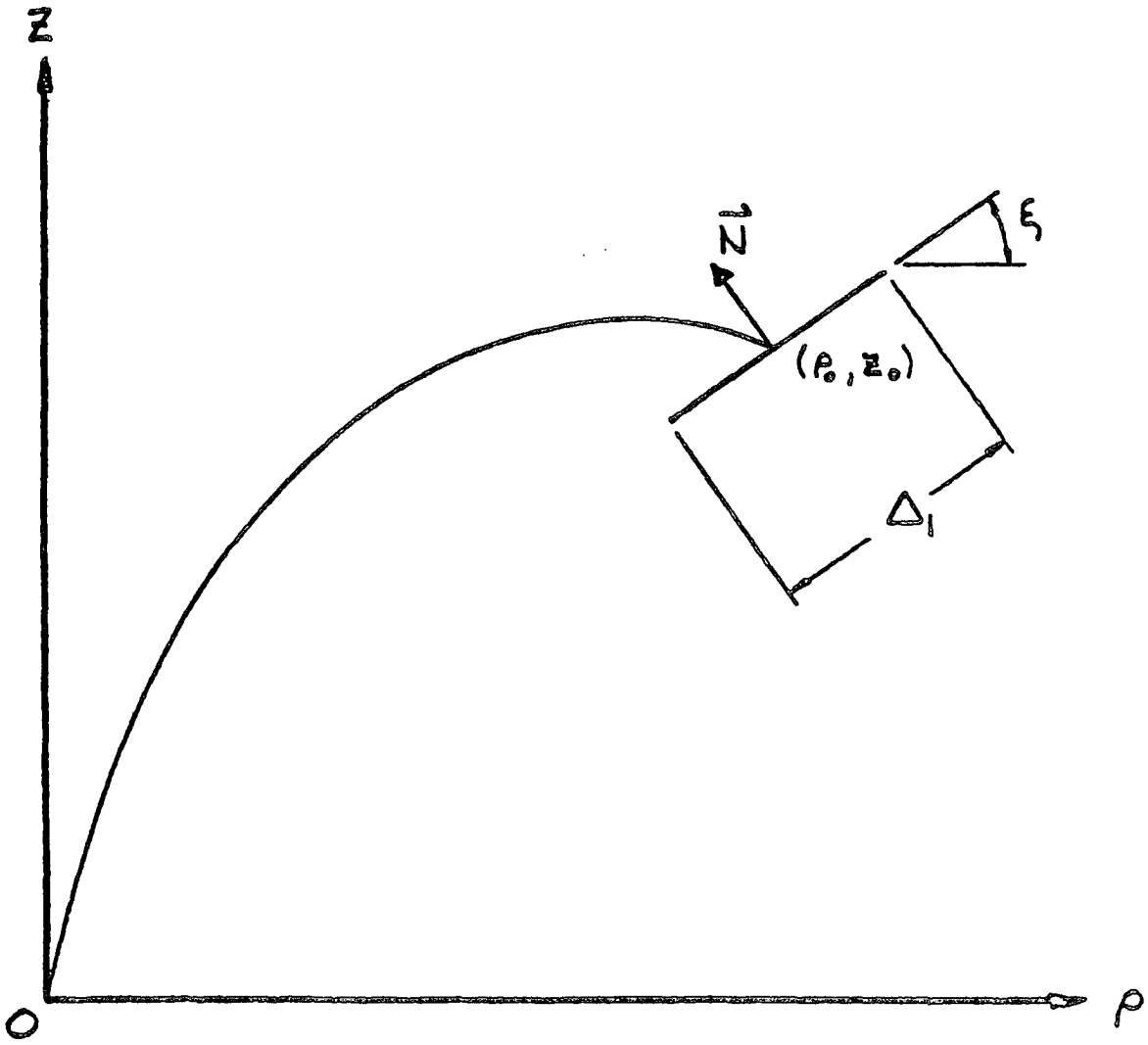

BYRON/BRAIDWOOD STATIONS
UPDATED FINAL SAFETY ANALYSIS REPORT

FIGURE C.2-4

STRIKE GEOMETRY IN TWO-DIMENSIONAL
ρ-Z PLANE

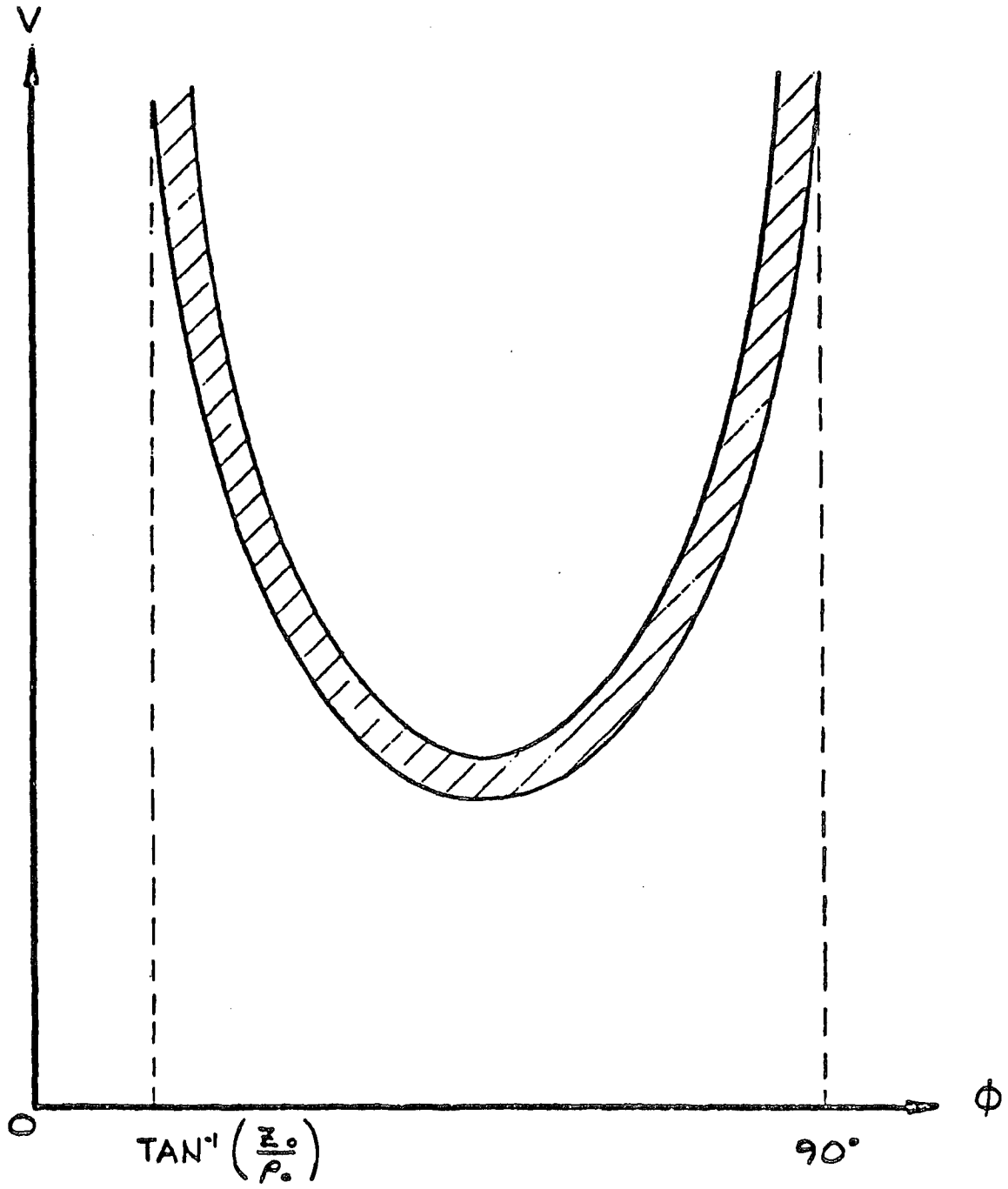

BYRON/BRAIDWOOD STATIONS
UPDATED FINAL SAFETY ANALYSIS REPORT

FIGURE C.2-5

THE BAND OF ALLOWED VALUES IN
THE ϕ-V PLANE

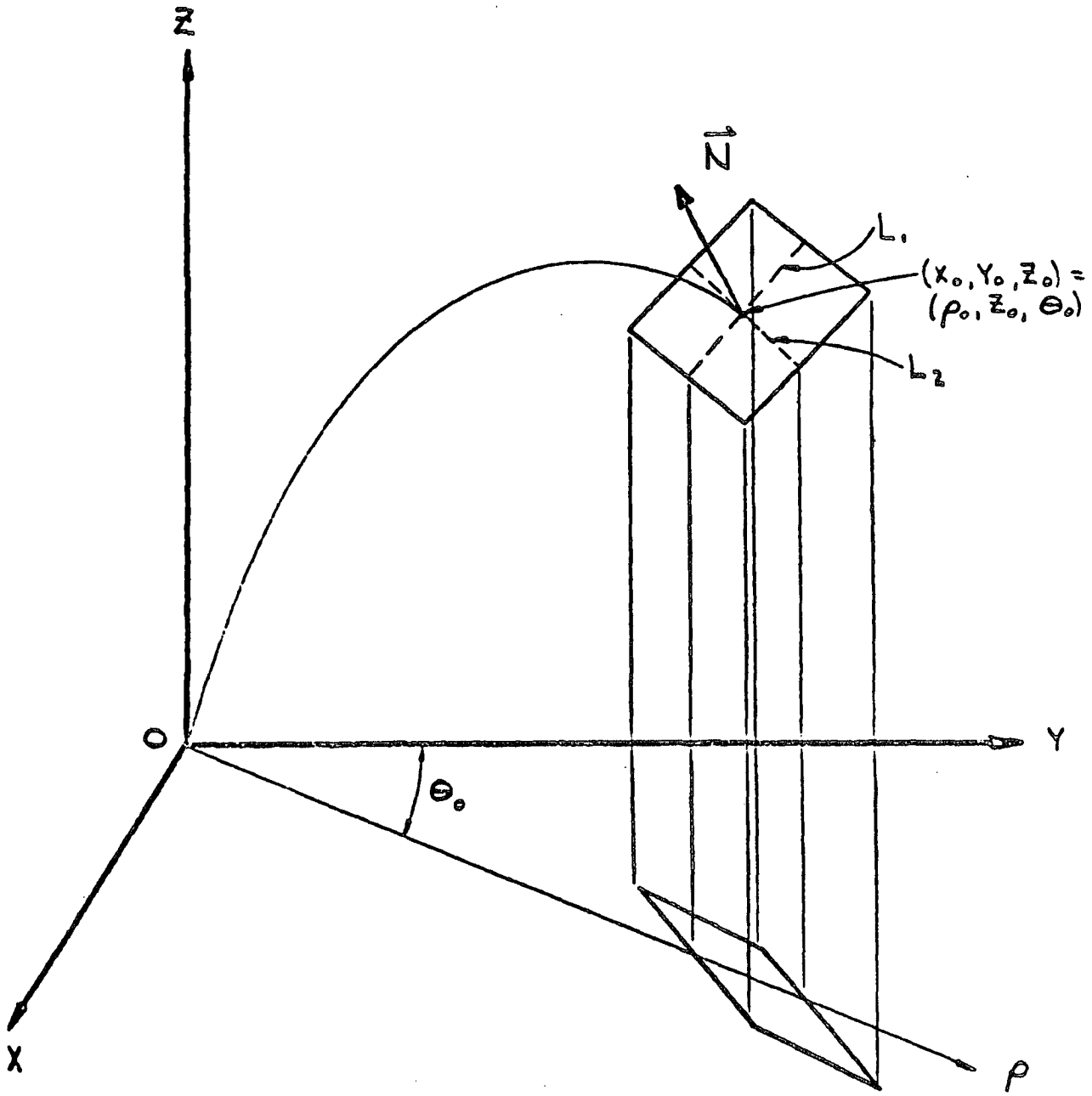

BYRON/BRAIDWOOD STATIONS
UPDATED FINAL SAFETY ANALYSIS REPORT

FIGURE C.2.6

STRIKE GEOMETRY IN X-Y-Z PLANE

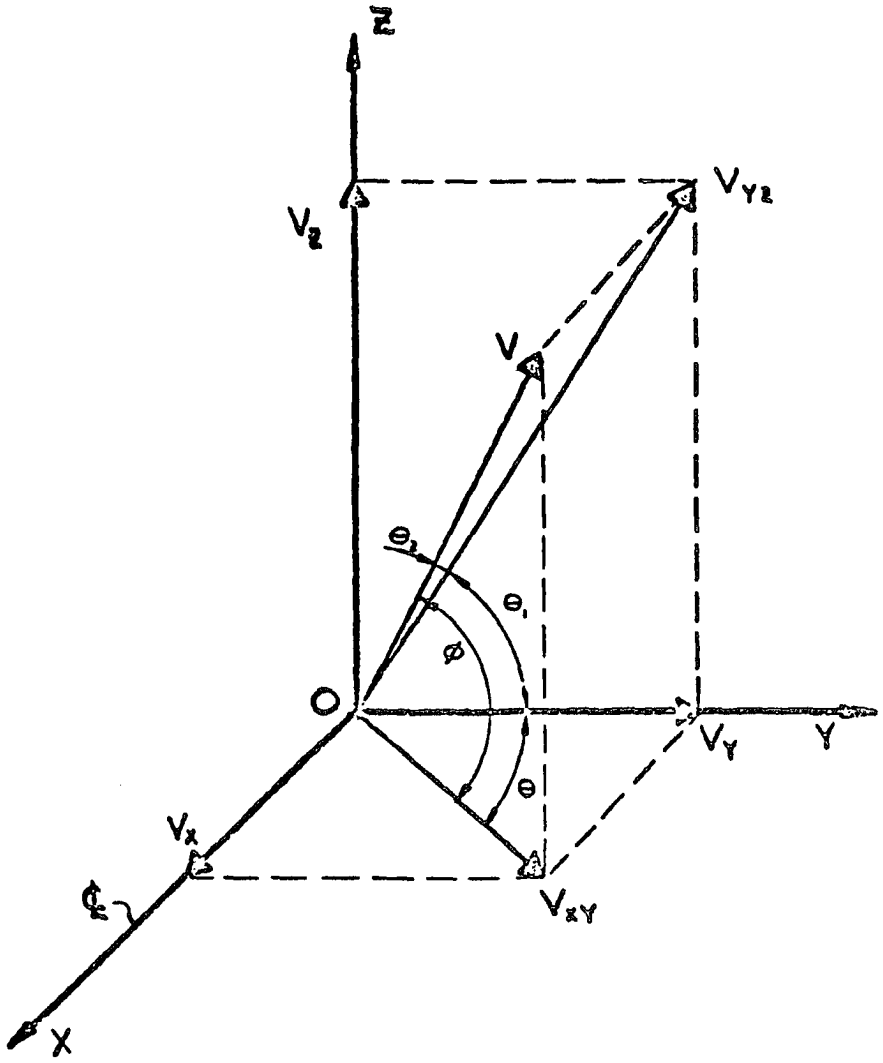

X AXIS = THE TURBINE AXIS
YZ - PLANE = THE DISC PLANE
XY - PLANE = THE HORIZONTAL PLANE

BYRON/BRAIDWOOD STATIONS
UPDATED FINAL SAFETY ANALYSIS REPORT

FIGURE C.2-7

RELATIONSHIP BETWEEN DISC PLANE
AND EXIT DIRECTION

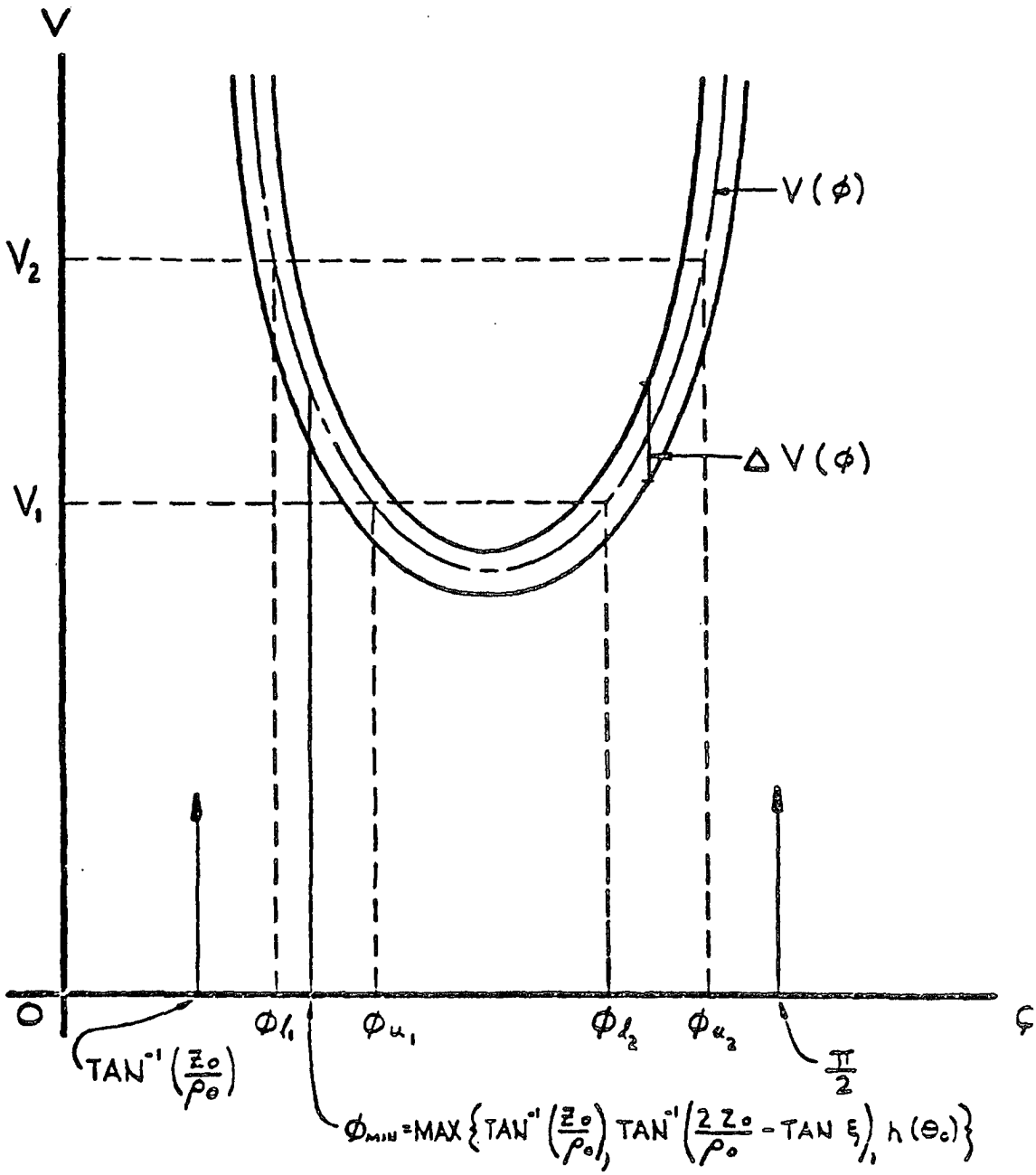

BYRON/BRAIDWOOD STATIONS
UPDATED FINAL SAFETY ANALYSIS REPORT

FIGURE C.2-8

LIMITS OF INTEGRATION OF THE INTEGRAL (24) OR INTEGRAL (30) AND THE RELATIONSHIP BETWEEN φ AND V

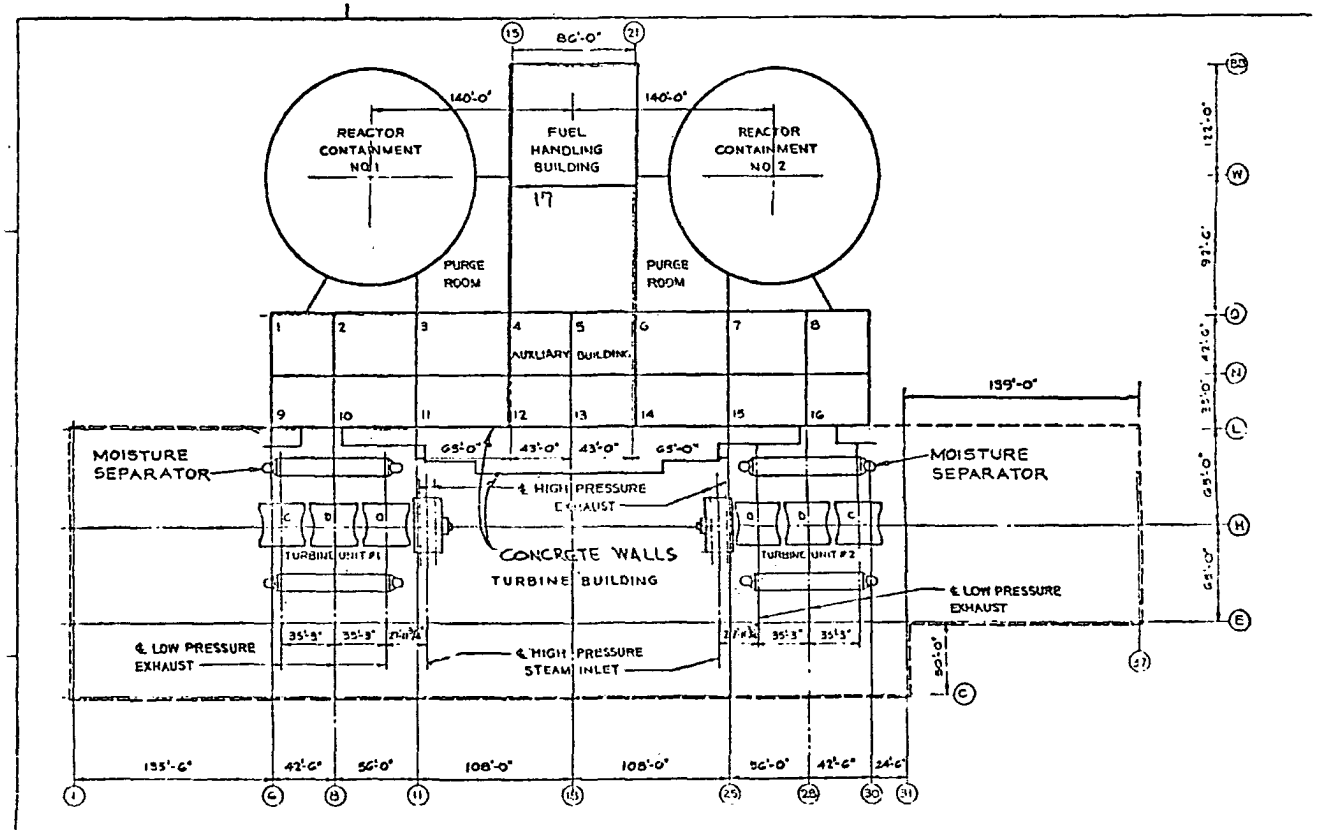

BYRON/BRAIDWOOD STATIONS
UPDATED FINAL SAFETY ANALYSIS REPORT

FIGURE C.3-1

PLANT ARRANGEMENT

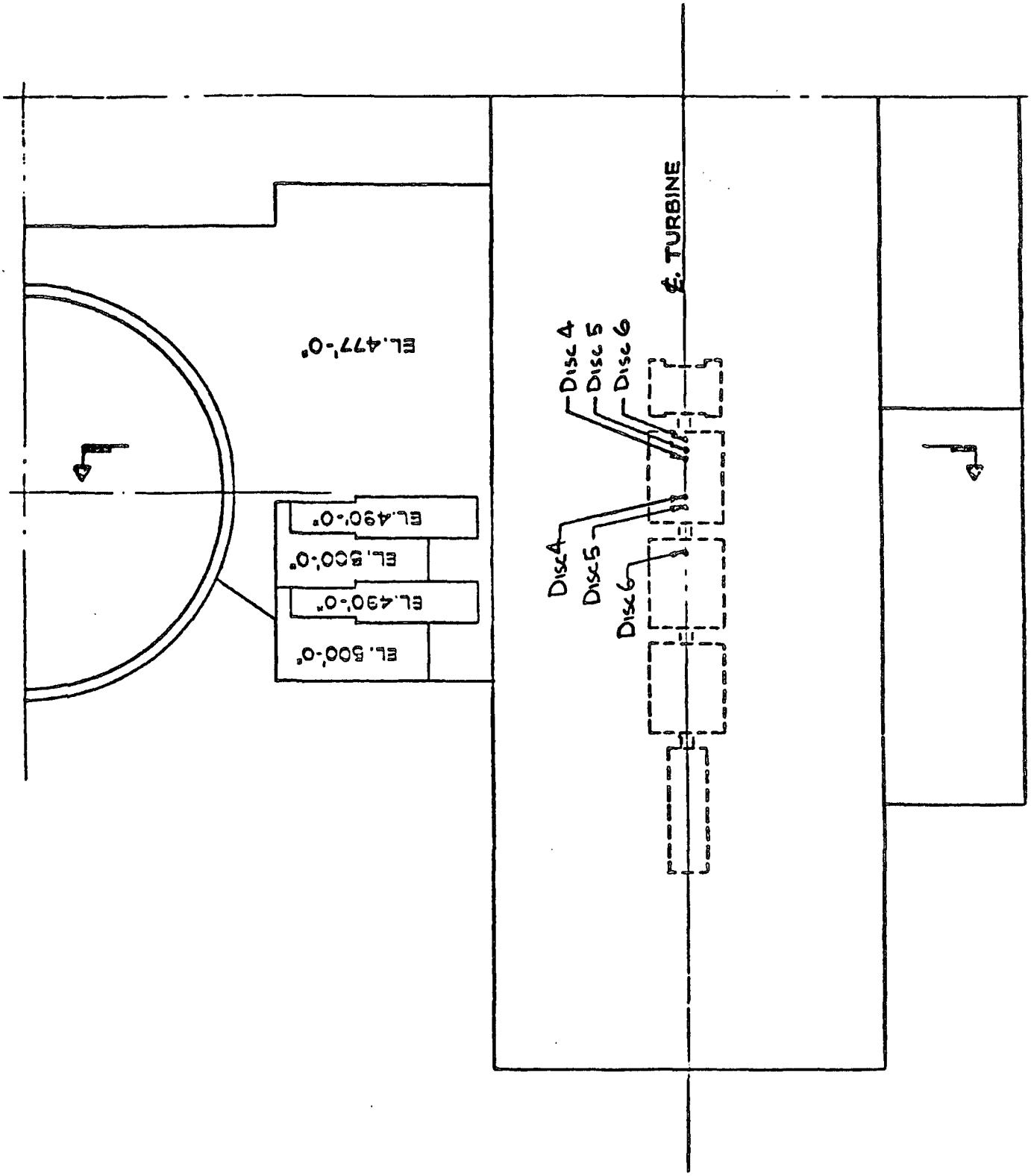

BYRON/BRAIDWOOD STATIONS
UPDATED FINAL SAFETY ANALYSIS REPORT

FIGURE C.A-1

CONTAINMENT AUXILIARY AND TURBINE
BUILDING ROOF PLAN

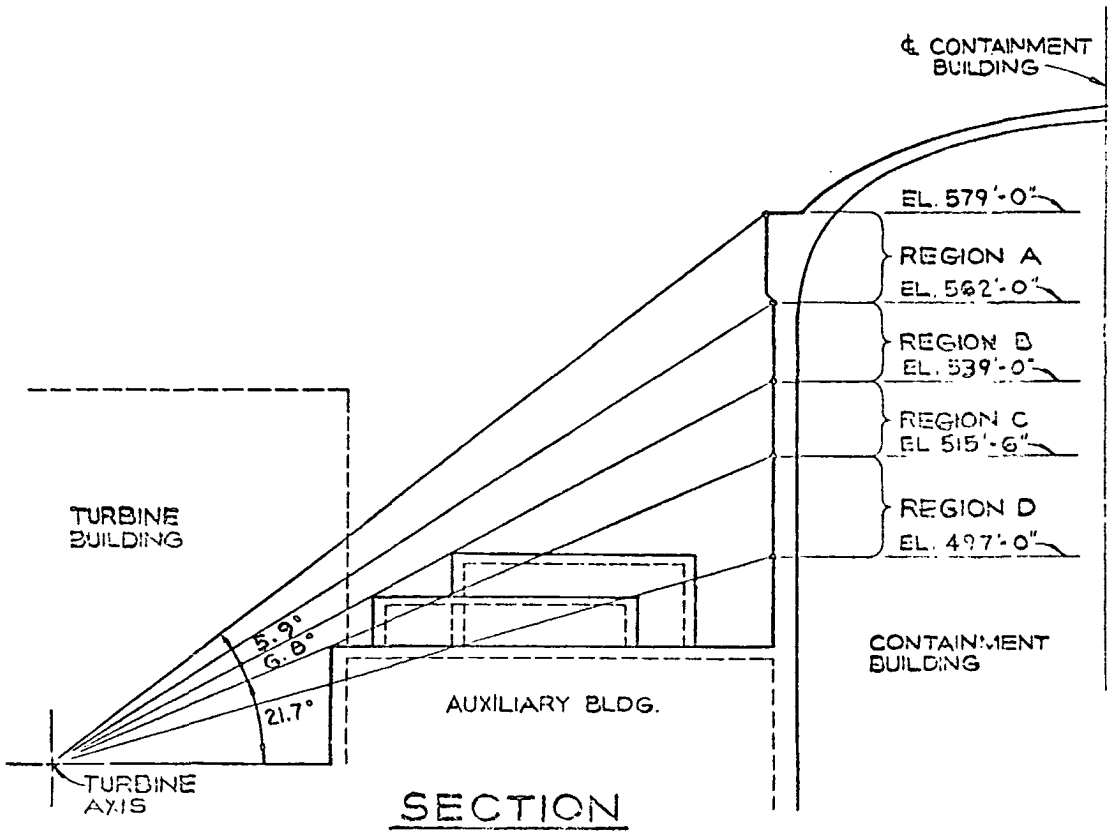

BYRON/BRAIDWOOD STATIONS UPDATED FINAL SAFETY ANALYSIS REPORT
FIGURE C.A-2 LOCATIONS OF REGIONS A, B, C, AND D ON CONTAINMENT BUILDING WALL

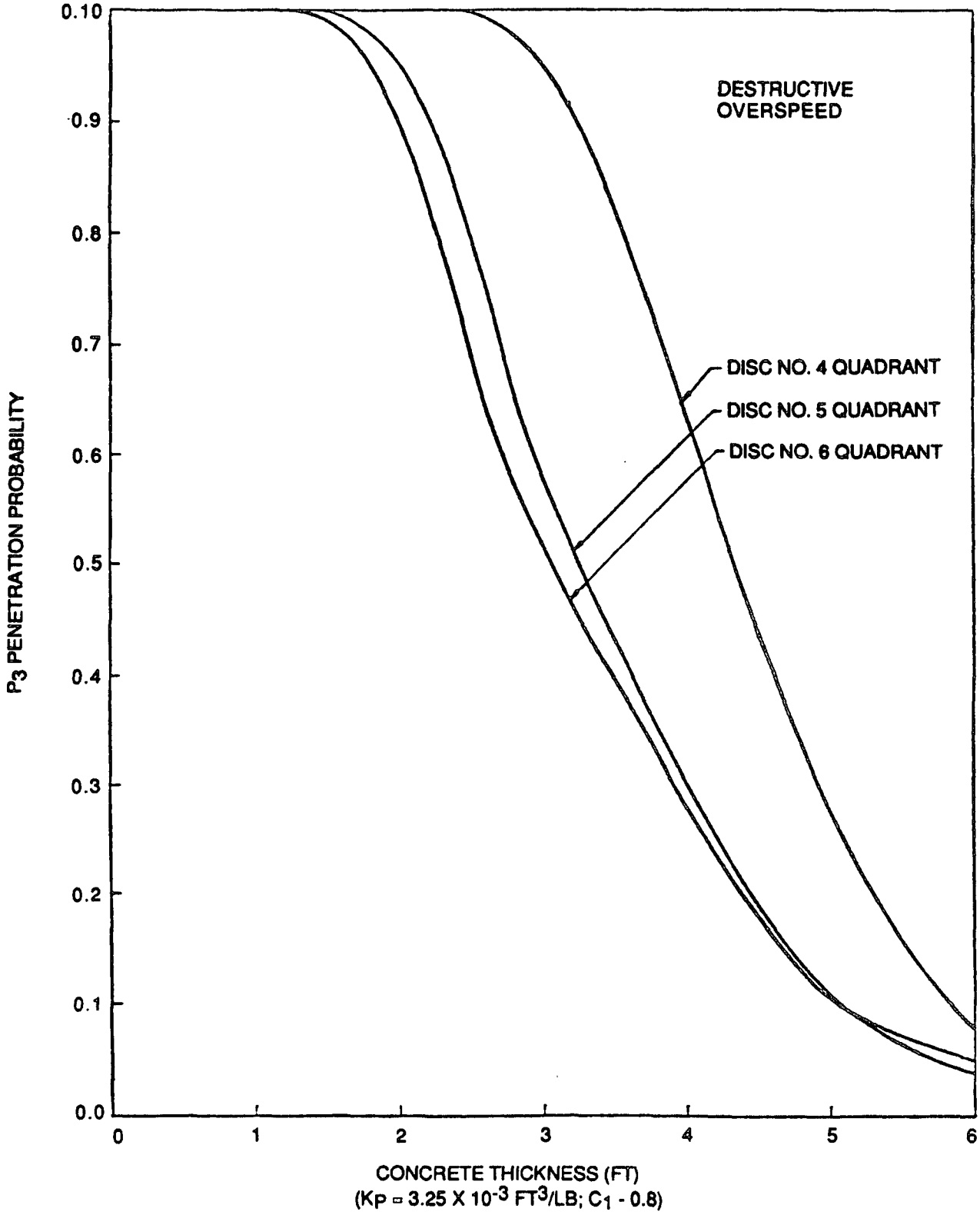

BYRON/BRAIDWOOD STATIONS
UPDATED FINAL SAFETY ANALYSIS REPORT

FIGURE C.A-3

P_3 VS. THICKNESS